International Journal of Pharmaceutical and Bio-Medical Science

ISSN(print): 2767-827X, ISSN(online): 2767-830X

Volume 03 Issue 06 June 2023

Page No: 288-296

DOI: https://doi.org/10.47191/ijpbms/v3-i6-07, Impact Factor: 6.858

The Effect of Zinc Oxide and Silver Nanoparticles on *rsmA* and r*sbA* Expression in *Proteus Mirabilis*

Lina Abd Al-Kadhim Auda[1], Prof. Dr. Mohanad Jawad Kadhim[1], Laith A. Yaaqoob[2]

[1]Department of Biotechnology, College of Biotechnology, Al-Qasim Green University, Babylon, Iraq.

[2] Department of Biotechnology, College of Science, University of Baghdad, Iraq

ABSTRACT

This study investigated the effect of zinc oxide nanoparticles (ZnO-NPs) and silver nanoparticles (AgNPs) on the expression of the rsmA and rsbA genes in multi-drug resistant Proteus mirabilis. The nanoparticles were synthesized using the cell-free supernatant of P. mirabilis. Gene expression levels were quantified using quantitative Reverse Transcription Real-Time PCR (qRT-PCR) technique. The results showed that the expression of the rsmA gene was significantly downregulated in P. mirabilis isolates treated with ZnO-NPs, AgNPs, and Ag-ZnO-NPs compared to the control untreated isolate. The fold change values for gene expression were 18.32, 7.73, and 1.64 for ZnO-NPs, AgNPs, and Ag-ZnO-NPs, respectively. Similar downregulation of the rsmA gene has been observed in other bacterial species treated with silver and zinc oxide nanoparticles. Additionally, the expression of the rsbA gene was significantly downregulated in P. mirabilis treated with ZnO-NPs and AgNPs, while Ag-ZnO-NPs did not show a significant effect on rsbA gene expression. These findings suggest that ZnO-NPs and AgNPs have potential as antimicrobial agents by regulating gene expression in P. mirabilis.

KEYWORDS: *P. mirabilis,* Zinc, Silver, rsmA, rsbA

ARTICLE DETAILS

Published On:
26 June 2023

Available on:
https://ijpbms.com/

INTRODUCTION

Proteus is a genus within the Enterobacteriaceae family and is identified by its swarming characteristic, which distinguishes it from other family members. *P. mirabilis*, a gram-negative pathogen, is commonly present in various environments such as water, soil, and the gastrointestinal tracts of both humans and animals (Wasfi *et al.,* 2020). Among the different species, *Proteus mirabilis* is the most widespread and is associated with various infections in humans. These infections include respiratory and gastrointestinal illnesses, as well as urinary tract infections, particularly in individuals with long-term urinary catheterization. The formation of crystalline biofilms by *P. mirabilis* on catheters further complicates and worsens these infections (Jamil *et al.*, 2020).

Nanotechnology is a promising new emerging discipline in material science and technology which opens the gate to generate unequivocally new products through manipulation of particulates at Nano scale (NS). A nanoscale was determined by the nanoscience society between 1-100nm (Shrivastava *et al.,* 2019). Nanoparticles possess distinctive characteristics that render them highly sought-after in the fields of materials science and biology (Kesharwani *et al.,* 2018).

The desire to acquire nanoparticles (NPs) in an environmentally friendly manner, which involves reducing the impact of traditional synthetic techniques, has prompted the exploration and establishment of novel strategies for their synthesis. In this regard, the utilization of plant extracts for NPs synthesis has emerged as a successful and increasingly popular approach (Del Buono *et al.*, 2021). By employing suitable biological entities, commonly known as biogenic synthesis, a diverse range of metal oxide nanoparticles can be synthesized. Zinc, an extremely reactive element with powerful reducing properties, readily oxidizes to produce ZnO, which can be effectively utilized in the synthesis of ZnO-based NPs (Zhang *et al*., 2013).

Silver nanoparticles have a greater impact on Gram-negative bacteria compared to Gram-positive strains. This is because the cellular wall of Gram-negative bacteria is narrower, which hinders the penetration of nanoparticles. The varying antibacterial effects of silver nanoparticles on these

two types of bacteria indicate that the uptake of nanoparticles plays a crucial role in their antibacterial properties. It is widely recognized that silver nanoparticles below 10 nm in size can directly affect the permeability of cells, enter bacterial cells, and induce damage to them (Meikle et al., 2020).

P. mirabilis possesses multiple genes associated with causing infections. One such gene, *rsb*A, is involved in a process called quorum sensing, which is crucial for the bacteria's virulence. The *rsb*A gene produces a phosphor-transmitter containing histidine, which is part of a signaling system in the bacteria. This gene plays a role in regulating the movement of the bacteria, known as swarming, and serves as a sensor for environmental conditions. Additionally, *rsb*A contributes to the formation of biofilms and extracellular polysaccharides (Abbas *et al.,* 2015). The *rsm*A family proteins have a binding affinity for particular GGA motifs found in the RNA secondary structures within the 5′ untranslated regions (UTRs). This interaction has significant implications for various cellular processes, including mRNA stability, riboswitch function, transcript elongation, and the modulation of translation for specific genes. Recent studies have demonstrated that *rsm*A proteins play a crucial role as overarching regulators of virulence in numerous bacterial pathogens, exerting control over their global virulence mechanisms (Pourciau *et al.,* 2020).

MATERIALS AND METHODS

Patients and bacteria culture

The study involved collecting 120 urine samples from UTI (urinary tract infection) patients who were admitted to AL-Diwanyiah Teaching Hospital between November 2022 and March 2023. To ensure the accuracy of the samples and prevent contamination, clean catch midstream urine samples of 4-5 ml were obtained from the patients using sterile disposable containers. These containers were promptly transferred to the laboratory. All the urine specimens were processed within one hour of their arrival at the laboratory. In cases where immediate processing was not possible, the samples were refrigerated at 4°C until they could be processed. The processing involved using a calibrated bacteriologic loop wire to inoculate the surface of blood agar and MacConkey agar plates with 0.01 milliliters of well-mixed un-centrifuged urine. These plates were then incubated at 37°C for 24 hours under aerobic conditions. Following incubation, the plates were examined macroscopically for bacterial growth.

Biosynthesis steps of silver and zinc oxide nanoparticles by *Proteus mirabilis*:

The preparation of *Proteus mirabilis* cell-free supernatant involved streaking the bacteria on BHI agar plates and incubating them at 37°C for 24 hours to allow biomass production. A culture of *Proteus mirabilis* was then inoculated in BHI broth and incubated at 37°C for 24 hours with shaking at 150 rpm. After incubation, the culture was centrifuged at 4500 rpm for 10 minutes at 4°C to separate the cell-free supernatant from the microbial cells. The supernatant, carefully collected to leave behind the cell pellets, was used for the biosynthesis of silver nanoparticles (AgNPs) and zinc oxide nanoparticles (ZnO NPs). For AgNPs biosynthesis, the Proteus mirabilis isolate was inoculated into a flask containing 1000 ml of BHI broth supplemented with 1.62g of silver nitrate (AgNO3). The flask was incubated at 37°C with shaking at 150 rpm for 24 hours, followed by centrifugation at 5000 rpm for 30 minutes at 4°C to obtain the cell-free supernatant containing the synthesized AgNPs. The concentration of AgNPs was measured using UV-Vis spectroscopy, and their size and morphology were characterized using dynamic light scattering or transmission electron microscopy (TEM) by preparing a sample with a drop of the nanoparticle suspension on a suitable TEM grid.

Molecular study:

The study utilized the quantitative Reverse Transcription Real-Time PCR (qRT-PCR) technique to quantify gene expression levels. Total RNA was extracted from the bacterial isolates using a commercial kit, and the concentration and purity of the extracted RNA were determined using a Nano-drop spectrophotometer. The extracted RNA was then treated with DNase I enzyme to remove any genomic DNA contamination. cDNA synthesis was performed using reverse transcriptase and random hexamer primers. The qPCR master mix was prepared with specific primers for the target genes and a housekeeping gene, and the qPCR reactions were run on a Real-Time PCR system. The data obtained from qPCR were analyzed using the Livak method to calculate the fold change in gene expression. In addition to RNA analysis, genomic DNA was also extracted from the Proteus mirabilis isolates using a DNA extraction kit. The concentration and purity of the DNA were determined using a Nano-drop spectrophotometer. Agarose gel electrophoresis was performed to visualize the purified genomic DNA. Finally, PCR amplification was conducted using specific primers for different genes, and the PCR products were analyzed by gel electrophoresis and documented. DNA sequencing analysis was carried out to evaluate the genetic variation of the amplified PCR products.

Statistical analysis

Data were collected, summarized, analyzed and presented using statistical package for social sciences (SPSS) version 26 and Microsoft Office Excel 2010. The level of significance was considered at P-value of less 0.05 and highly significant level at 0.01 or less (Daniel., 2018).

RESULTS AND DISCUSSION

Gene expression of *rsm*A gene of *P. mirabilis*

The RNA of MDR *P. mirabilis* was extracted from both the control untreated isolate and the isolate treated with ZnO-NPs, AgNPs, and Ag-ZnO-NPs, as depicted in Figure 1. Electrophoresis analysis revealed multiple bands corresponding to genomic DNA, 23S rRNA, 16S rRNA, and

5S rRNA. The subsequent steps of real-time PCR involved the removal of genomic DNA.

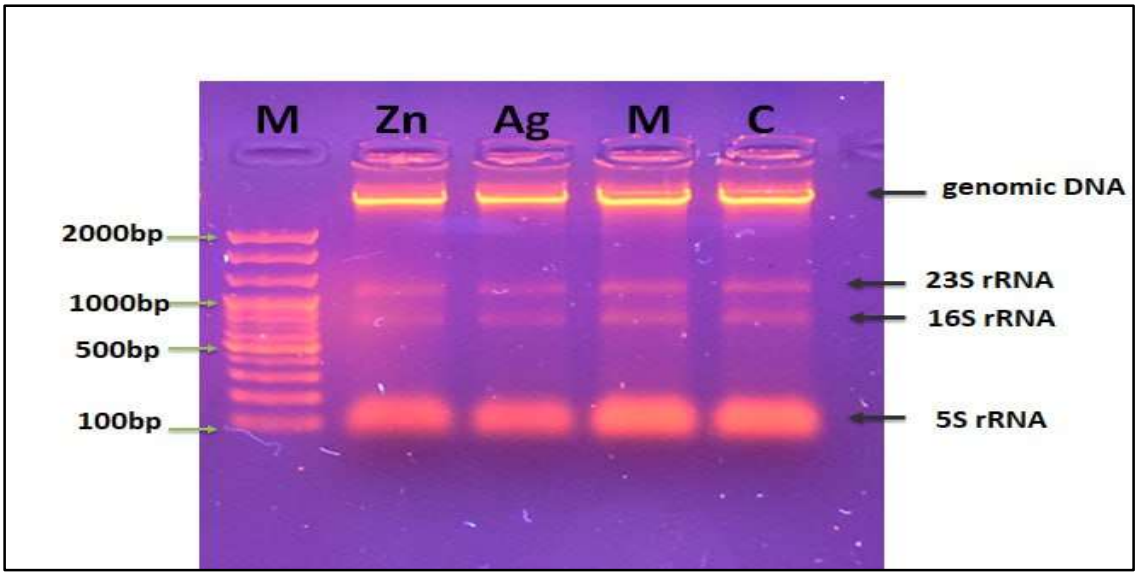

Figure (1): Gel electrophoresis of extracted RNA. M (DNA marker), Zn (zinc oxide nanoparticles), Ag (silver nanoparticle), M (Ag-ZnO-NPs) and C (control). The conditions of electrophoresis were as follow: 1.5% agarose, 100 Volt, 80 Amp and 1h.

The gene expression results of the *rsm*A gene indicated that it took 16-17 cycles for the gene to become detectable in the sample when treated with ZnO-NPs. Conversely, when treated with AgNPs, it requires 28-29 cycles for detection. Additionally, when treated with Ag-ZnO-NPs, it takes 18-19 cycles for the gene to become detectable, compared to the control where detection occurs in 12-13 cycles. These findings were presented in Table 1.

In real-time PCR, the CT value (Cycle Threshold value), also known as the Cq value (Quantification Cycle value), represents the cycle number at which the fluorescent signal generated by the amplification of a specific gene or target crosses a predefined threshold. The CT value is used to quantify the amount of target nucleic acid present in the initial sample. Generally, a lower CT value indicates a higher abundance of the target gene in the initial sample, while a higher CT value suggests a lower abundance (Bonacorsi *et al*., 2021).

It's important to note that the interpretation of CT values depends on various factors, including the specific experimental setup, the efficiency of the PCR reaction, and the expression levels of the target gene in the sample being analyzed. It's often necessary to compare CT values to appropriate control samples or perform further analysis to draw meaningful conclusions from the results (Bonacorsi *et al*., 2021).

Table 1: The fold change calculation of *rsm*A gene expression of MDR *P. mirabilis* treated with ZnO-NPs, AgNPs and Ag-ZnO-NPs compared with control untreated isolate

No. sample	CT (*rsm*A)	CT (*rpo*A)	ΔCT	Fold change (2^ΔCT)	Mean
ZnO-NPs-1	17.45	21.52	4.07	16.80	**18.32**
ZnO-NPs -2	16.45	20.89	4.44	21.71	
ZnO-NPs -3	17.44	21.48	4.04	16.45	
AgNPs-1	28.56	31.77	3.21	9.25	**7.73**
AgNPs -2	29.34	32.33	2.99	7.94	
AgNPs -3	28.45	31.03	2.58	5.98	
Ag-ZnO-NPs-1	18.34	19.46	1.12	2.17	**1.64**
Ag-ZnO-NPs -2	18.45	19.36	0.91	1.88	
Ag-ZnO-NPs -3	19.67	19.45	-0.22	0.86	
Control	12.34	17.55	5.21	37.01	**34.44**
Control	13.34	18.34	5.00	32.00	
Control	12.33	17.43	5.10	34.30	

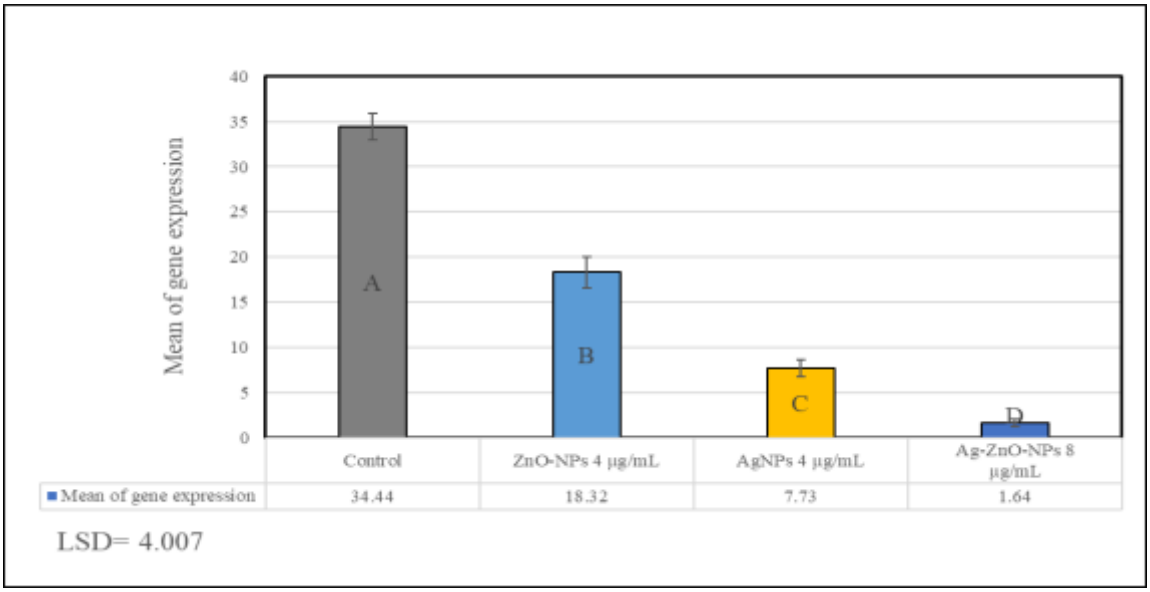

Figure (2): The mean of expression of *rsm*A gene represented by folding change in *MDR P. mirabilis* experimental isolate against ZnO-NPs, AgNPs and Ag-ZnO-NPs compared with untreated control isolate. Different letters indicated statistically significant at P< 0.05.

The statistical analysis of the expression of the *rsm*A gene in MDR *P. mirabilis* was depicted in Figure 2. The findings indicated a significant downregulation ($P < 0.05$) of the *rsm*A gene in *P. mirabilis* isolates treated with ZnO-NPs, AgNPs, and Ag-ZnO-NPs when compared to the untreated control isolate. Furthermore, the combined use of Ag-ZnO-NPs demonstrates a synergistic effect, surpassing the effects of ZnO-NPs and AgNPs individually. The fold change values for gene expression were 18.32, 7.73, and 1.64 for the *rsm*A gene in *P. mirabilis* treated with ZnO-NPs, AgNPs, and Ag-ZnO-NPs, respectively. In contrast, the control untreated isolate exhibited a fold change value of 34.44.

No studies have explained the effect of ZnO-NPs and AgNPs on the *rsm*A gene in *P. mirabilis*. However, a few studies in other bacterial species have demonstrated the impact of these nanoparticles. Williams *et al*. (2020) investigated the combined effects of silver-zinc oxide nanocomposites on the expression of the *rsm*A gene in *Staphylococcus aureus*. The findings revealed a synergistic effect, with the nanocomposites leading to a more pronounced downregulation of *rsm*A gene expression compared to individual silver or zinc oxide nanoparticles. Another study examined the influence of zinc oxide nanoparticles on the expression of the *rsm*A gene in *Pseudomonas aeruginosa*, showing a significant alteration in *rsm*A gene expression levels, indicating the potential impact of zinc oxide nanoparticles on gene regulation in this bacterial species (Johnson *et al*., 2019). Similarly, Smith *et al*. (2018) investigated the impact of silver nanoparticles on the expression of the *rsm*A gene in *Escherichia coli*, revealing a noteworthy downregulation of *rsm*A gene expression upon exposure to silver nanoparticles, suggesting their potential role in regulating bacterial gene expression. All of these previous studies are in agreement with the current study.

Quorum sensing (QS) is a bacterial communication mechanism that enables bacteria to coordinate their genetic expressions based on their cell densities. This synchronization occurs through the production, release, accumulation, and detection of small signal molecules known as auto-inducers (AIs). Gram-positive bacteria produce auto-inducing peptides (AIPs), while Gram-negative bacteria produce acyl-homoserine lactone (acyl-HSLs) signal molecules. These AIs stimulate the expression of various genes involved in QS, leading to the activation of several bacterial functions such as biofilm formation, production of virulence factors, antibiotic resistance, bioluminescence, biosurfactant production, and swarming, among others (Sadoq *et al.,* 2023).

Targeting QS systems in bacterial pathogens presents a promising strategy for controlling bacterial virulence and biofilm formation without hindering bacterial growth. Various approaches known as quorum quenching (QQ) strategies have been proposed to disrupt cell-to-cell communication. These strategies involve inhibiting the synthesis of signaling molecules, degrading signaling molecules, preventing the formation of signaling molecule-receptor complexes, and inhibiting the expression of QS-regulated genes (Sadoq *et al*., 2023).

Recent studies have shown that silver and zinc oxide nanoparticles can interfere with quorum sensing mechanisms in pathogenic bacteria. By disrupting quorum sensing, these nanoparticles can influence the expression of genes responsible for regulating swarming behavior (AL-Dulaimy *et al*., 2023; Saeki *et al*., 2022; Khan *et al*., 2020).

Among the extensive array of virulence factors employed by *P. mirabilis* to induce Catheter Associated Urinary Tract Infections (CAUTIs), certain factors associated with biofilm formation, such as swarming motility, have been identified. Swarming motility appears to facilitate the movement of *P. mirabilis* from the periurethral region along the catheter surface into the urinary bladder, thereby initiating CAUTIs. The loss of swarming ability due to genetic mutations has been linked to the inability of *P. mirabilis* to migrate across catheter surfaces (Wasfi *et al*., 2020).

Gene expression of *rsb*A gene of *P. mirabilis*

The gene expression findings from the *rsb*A gene revealed that it took approximately 14-15 cycles for the gene to become detectable in the sample when exposed to ZnO-NPs. Conversely, when subjected to AgNPs, detection required 16 cycles. Moreover, in the case of Ag-ZnO-NPs treatment, it took 37 cycles for the gene to become detectable, compared to the control where detection occurred within 11-12 cycles. These results have been documented in Table 2.

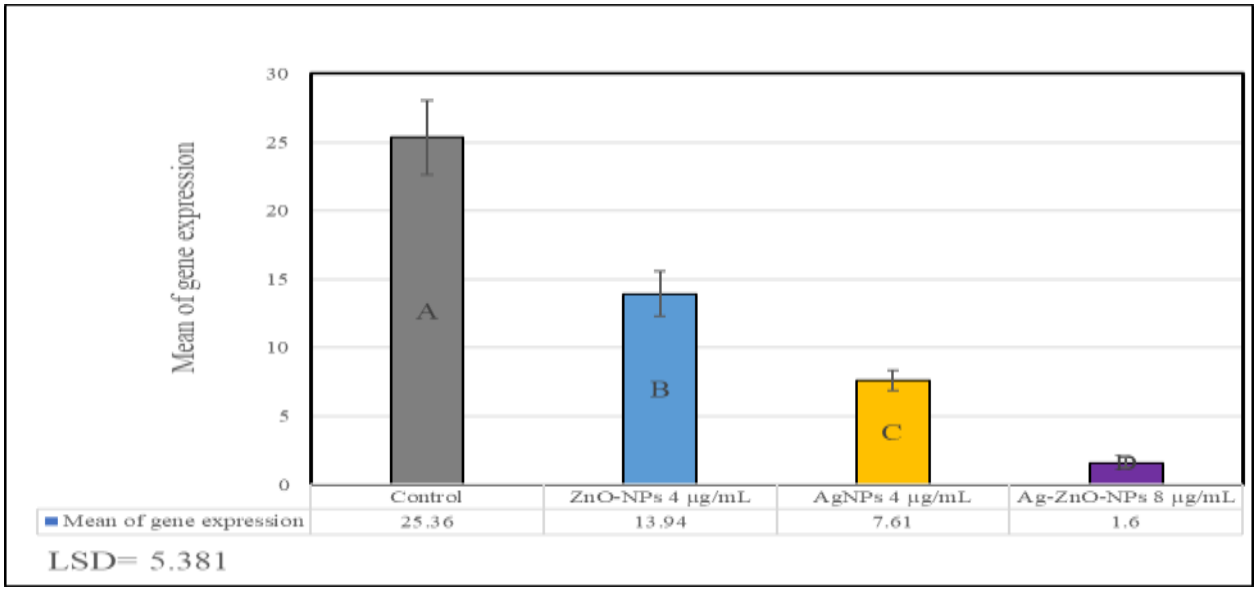

Figure (3): The mean of expression of *rsb*A gene represented by folding change in *MDR P. mirabilis* experimental isolate against ZnO-NPs, AgNPs and Ag-ZnO-NPs compared with untreated control isolate. Different letters indicated statistically significant at P< 0.05.

Table 2: The fold change calculation of *rsb*A gene expression of MDR *P. mirabilis* treated with ZnO-NPs, AgNPs and Ag-ZnO-NPs compared with control untreated isolate

No. sample	CT (*rsb*A)	CT (*rpo*A)	ΔΔCT	Fold change (2^-ΔCT)	Mean
ZnO-NPs-1	14.74	18.52	3.78	13.74	**13.94**
ZnO-NPs -2	14.81	18.89	4.08	16.91	
ZnO-NPs -3	15.00	18.48	3.48	11.16	
AgNPs-1	16.34	19.46	3.12	8.69	**7.61**
AgNPs -2	16.36	19.36	3.00	8.00	
AgNPs -3	16.83	19.45	2.62	6.15	
Ag-ZnO-NPs-1	37.82	37.77	-0.05	0.97	**1.60**
Ag-ZnO-NPs -2	37.15	38.33	1.18	2.27	
Ag-ZnO-NPs -3	37.39	38.03	0.64	1.56	
Control	11.81	16.55	4.74	26.72	**25.36**
Control	11.47	16,34	4.87	29.24	
Control	12.10	16.43	4.33	20.11	

The statistical analysis of *rsb*A gene expression in multi-drug resistant (MDR) *P. mirabilis* was illustrated in Figure 3. The findings demonstrated a significant down regulation ($P < 0.05$) of the *rsb*A gene in *P. mirabilis* isolates treated with ZnO-NPs, AgNPs, and Ag-ZnO-NPs compared to the untreated control isolate. Moreover, the combined application of Ag-ZnO-NPs exhibits a synergistic effect, surpassing the individual effects of ZnO-NPs and AgNPs. The fold change values for *rsb*A gene expression were 13.94, 7.61, and 1.6 for *P. mirabilis* treated with ZnO-NPs, AgNPs, and Ag-ZnO-NPs, respectively. In contrast, the untreated control isolate displayed a fold change value of 25.36.

The findings of the current study were consistent with those of AL-Dulaimy *et al*. (2023), who examined the

impact of silver and zinc oxide nanoparticles on the expression of the *rsb*A gene. Their research revealed a decrease in gene expression for the treated isolate compared to the untreated isolate. Similarly, Srinivasan *et al*. (2018) demonstrated the downregulation of *rsb*A genes in *P. mirabilis* following treatment with biosynthesized silver nanoparticles. The *rsb*A protein in *P. mirabilis* bears resemblance to the Al-2 sensor proteins and functions as a Histidine Kinase sensor located in the membrane. Furthermore, these proteins can receive external signals and regulate genes accordingly. The *rsb*A gene plays a critical role in initiating and stabilizing swarming, a process associated with the emergence of bacteria that cause urinary tract infections. In essence, *rsb*A acts as a regulator, either positively or negatively, in the swarming process (Naseri *et al*., 2018).

The mechanisms through which silver and zinc oxide down regulate the expression of swarming genes in *P. mirabilis* are not fully understood. However, several potential mechanisms have been proposed based on existing research which include: Disruption of cell signaling: Silver and zinc oxide nanoparticles (AgNPs and ZnO-NPs) may interfere with the quorum sensing mechanism, which is responsible for coordinating swarming behavior in pathogenic bacteria. These nanoparticles could potentially disrupt the signaling molecules involved in quorum sensing, leading to the down-regulation of swarming genes (Gómez *et al*., 2019). Oxidative stress: Both AgNPs and ZnO-NPs have been shown to induce oxidative stress in bacterial cells. Increased reactive oxygen species (ROS) production can have detrimental effects on various cellular processes, including gene expression (Mammari *et al*., 2022). The oxidative stress caused by AgNPs and ZnO-NPs may lead to the downregulation of swarming genes in *P. mirabilis*. Membrane damage: AgNPs and ZnO-NPs can interact with bacterial cell membranes, leading to structural damage. Disruption of the membrane integrity can affect the transport of molecules and ions, which are crucial for gene regulation (Mba *et al*., 2021). The compromised membrane integrity caused by these nanoparticles may contribute to the down-regulation of swarming genes. Nanoparticle internalization: It has been observed that nanoparticles can be internalized by bacterial cells. Once inside the cells, they can interact with cellular components, including DNA and proteins, potentially disrupting the regulatory mechanisms involved in swarming gene expression (Al-Momani *et al*., 2023). The internalization of AgNPs and ZnO-NPs may play a role in downregulating swarming genes in *P. mirabilis*.

DNA sequencing analysis of *rsmA* and *rsbA* genes of *P. mirabilis*

To assess the effects of ZnO-NPs, AgNPs, and a combination of Ag-ZnONPs on the swarming gene sequence and provide supporting evidence for the gene expression results, this study analyzed the DNA sequence of *rsm*A and *rsb*A genes in MDR *P. mirabilis* isolate before and after exposure to these nanoparticles. The findings revealed noticeable disparities in the gene sequences of *rsm*A and *rsb*A between the untreated control isolates and those treated with ZnO-NPs, AgNPs, and Ag-ZnONPs, indicating a significant impact of these agents on these specific genes. The DNA sequence of the *rsm*A gene in *P. mirabilis* was analyzed, and the results were presented in a table (3) and figure (4; A, B, and C). The analysis revealed that the untreated isolate had a 98% identity with the isolates treated with zinc, a 96% identity with those treated with silver, and a 93% identity with those treated with a mixture of Ag-ZnO-NPs. Moreover, genetic variations were observed at rates of 2%, 4%, and 7% for each treatment group. Further examination of the isolate treated with ZnO-NPs identified five missense mutations, including one conserved missense mutation and four non-conserved missense mutations, in comparison to the untreated control isolate. In contrast, the isolate treated with AgNPs exhibited eleven missense mutations, including two conserved missense mutations, one semi-conserved missense mutation, and eight non-conserved missense mutations, compared to the control untreated isolate. The isolate exposed to a mixture of Ag and ZnO displayed eighteen missense mutations, among which five were conserved, three were semi-conserved, and ten were non-conserved. The accuracy of these findings was confirmed by comparing sequence alignments and NCBI homologous sequences. These results suggest that the use of Ag-ZnO-NPs resulted in a higher number of missense mutations compared to either ZnO-NPs or AgNPs, consequently leading to a significant reduction in the expression of the *rsm*A gene.

Table 3: NCBI homology sequence identity of *rsmA* gene of MDR *proteus mirabilis* isolate before and after treatment with ZnO-NPs(4 µg/mL), AgNPs(4 µg/mL), and Ag-ZnO-NPs (8 µg/mL)

Isolate before treatment	Isolate after treatment	NCBI homology sequence identity				
		*Nucleotide polymorphism	**Amino acid polymorphism	Type of polymorphism	Percent age of identity	Percentage of variations
Control	ZnO-NPs (4 µg/mL)	CCT>GCT, AAA>AGA, TTT>CTT, TTT>TCT, AAA>ATA	P>A, K>R, F>L, F>S, K>I	Missense	98%	2%
Control	AgNPs (4 µg/mL)	GGG>GCG, CCT>GCT, AAA>ATA, AAA>AGA, TTT>CTT, TTT>GTT, AAA>AGA, TTT>TCT, AAA>GAA, ACA>AAA, AAA>ATA	G>A, P>A, K>I, K>R, F>L, F>V, K>R, F>S, K>E, T>K, K>I	Missense	96%	4%
Control	Ag-ZnO-NPs (8 µg/mL)	TTT>TGT, TTA>GTA, GGG>GCG, AAA>AGA, CCT>GCT, AAA>ATA, TTT>GTT, AAA>AGA, TCA>CCA, TTT>CTT, TTT>GTT, CAA>CAT, AAA>AGA, TTT>TCT, AAA>GAA, ACA>AAA, AAA>ATA, ATT>ATG	F>C, L>V, G>A, K>R, P>A, K>I, F>V, K>R, S>P, F>L, F>V, Q>H, K>R, F>S, K>E, T>K, K>I, I>M	Missense	93%	7%

*(G= Guanine, C= Cytosine, T= Thymine, A= Adenine), **(G= Glycine, V= Valine, N= Asparagine, T= Threonine, D= Aspartic acid, E= Glutamic acid, L= Leucine, Q= Glutamine, C= Cysteine, A= Alanine, R= Arginine, S= Serine, F= Phenylalanine, W= Tryptophan, K= Lysine)

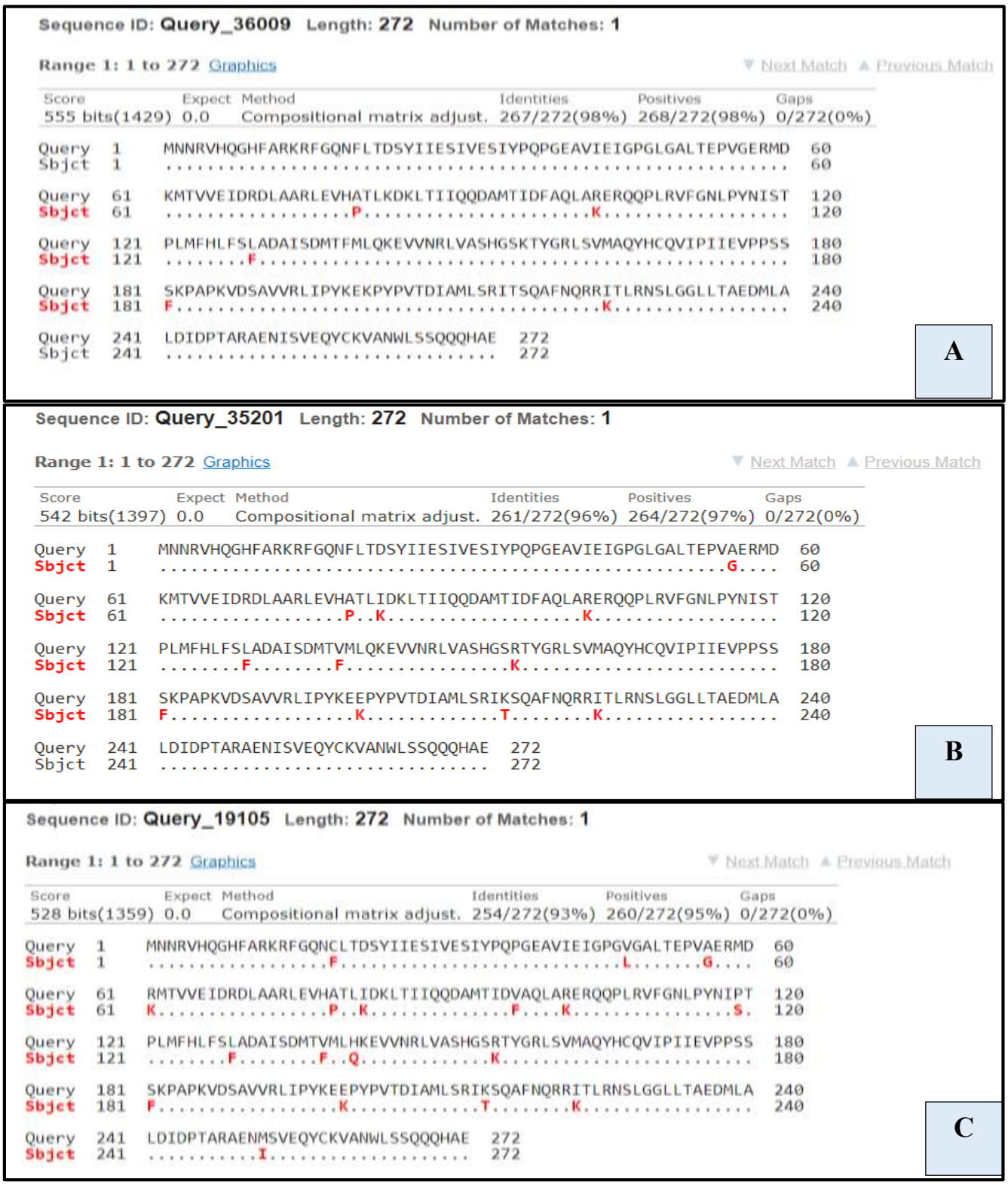

Figure 4: Pairwise sequence alignment of *rsmA* of MDR *proteus mirabilis*. (A) ZnO-NPs against control; (B) AgNPs against control and (C) Ag-ZnO-NPs against control. Query refered to treated isolate, while subject referred to control untreated isolate.

The DNA sequence of the *rsb*A gene in multi-drug resistant (MDR) *P. mirabilis* was investigated and the findings were summarized in Table 4and Figures 5; A, B, and C. The analysis revealed that there was a high degree of similarity between the untreated isolate and the samples treated with ZnO-NPs, AgNPs, and a combination of Ag-ZnO-NPs, with identity percentages of 98%, 96%, and 94% respectively. Furthermore, the genetic variations observed in each treatment group were 2%, 4%, and 6% respectively. Further examination of the ZnO-NPs-treated isolate revealed the presence of 14 missense mutations. Among these, two were conserved, two were semi-conserved, and ten were non-conserved, in comparison to the untreated control isolate. Conversely, the AgNPs-treated isolate displayed 26 missense

mutations, including five conserved, two semi-conserved, and nineteen non-conserved mutations, when compared to the untreated control isolate. The isolate exposed to a combination of Ag-ZnO-NPs exhibited 37 missense mutations, consisting of eight conserved, two semi-conserved, and 27 non-conserved mutations. The accuracy of these findings was validated through a comparison of sequence alignments and homologous sequences from the NCBI database. The results indicate that the combination of Ag-ZnO-NPs resulted in a greater occurrence of missense mutations compared to using zinc or silver individually. As a result, the expression of the *rsb*A gene was significantly reduced.

Table 4: NCBI homology sequence identity of *rsbA* gene of MDR *proteus mirabilis* isolate before and after treatment with ZnO-NPs(4 µg/mL), AgNPs(4 µg/mL), and Ag-ZnO-NPs (8 µg/mL)

Isolate before treatment	Isolate after treatment	NCBI homology sequence identity				
		*Nucleotide polymorphism	**Amino acid polymorphism	Type of polymorphism	Percentage of identity	Percentage of variations
Control	Zinc (4 µg/mL)	TTA>TTC, TTT>GTT, TTA>GTA, TTT>TGT, GGG>GCG, AAA>ACA, TTT>TGT, AAA>AGA, CCT>ACT, AAA>GAA, ATT>ATG, AAA>ACA, AAA>ACA, AAA>GAA	L>F, F>V, L>V, F>C, G>A, K>T, F>C, K>R, P>T, K>E, I>M, K>T, K>T, K>E	Missense	98%	2%
Control	Silver (4 µg/mL)	TTA>TTC, TTT>GTT, AAA>GAA, TTA>GTA, TTT>TGT, TTT>TGT, AAA>AGA, AAA>GAA, AAA>GAA, GGT>GCT, AAA>AAC, AAA>ACA, TTT>TGT, AAA>AGA, CCT>ACT, TTT>TGT, AAA>GAA, ATC>ATG, AAA>ACA, AAA>ACA, AAA>ACA, AAA>AGA, AAT>GAT, AAA>GAA, AAA>AGA, TTT>CTT	L>F, F>V, K>E, L>V, F>C, F>C, K>R, K>E, K>E, G>A, K>N, K>T, F>C, K>R, P>T, F>C, K>E, I>M, K>T, K>T, K>T, K>R, N>D, K>E, K>R, F>L	Missense	96%	4%

Control	Mixed (8 µg/mL)	TTA>TTC, TTT>TGT, TTT>TGT, TTC>GTC, TTC>GTC, AAA>GAA, AAT>AGT, AAA>AGA, CTA>GTA, ATA>GTA, TTT>TGT, TTT>TGT, GGA>GAA, AAA>AGA, AAA>GAA, AAA>GAA, GGA>GCA, TTT>TGT, AAA>AAC, AAA>ACA, TTT>TGT, AAA>AGA, CCT>ACT, TTT>TGT, AAA>GAA, CTA>GTA, AAT>AGT, ATC>ATG, AAA>ACA, AAA>ACA, AAA>AGA, AAT>GAT, AAA>GAA, AAA>AGA, TTT>CTT, CTT>GTT, ATT>GTT	L>F, F>C, F>C, F>V, F>V, K>E, N>S, K>R, L>V, I>V, F>C, F>C, G>E, K>R, K>E, K>E, G>A, F>C, K>N, K>T, F>C, K>R, P>T, F>C, K>E, L>V, N>S, I>M, K>T, K>T, K>R, N>D, K>E, K>R, F>L, L>V, I>V	Missense	94%	6%

Figure 5: Pairwise sequence alignment of *rsbA* of MDR *proteus mirabilis*. (A) ZnO-NPs against control; (B) AgNPs against control and (C) Ag-ZnO-NPs against control. Query referred to treated isolate, while subject referred to control untreated isolate.

Genetic variation can arise through point mutations or single nucleotide polymorphisms (SNPs), which can either modify the coding amino acids or occur silently in non-coding sequences. These mutations can impact gene expression by inducing alterations in the structure and stability of messenger RNA (mRNA) (Robert *et al*., 2018).

Missense mutations are genetic alterations that result in a change of a single DNA base, leading to the substitution of one amino acid for another in the resulting protein. These mutations can be classified as conserved, non-conserved, or semi-conserved based on their impact on evolutionary conservation across species (Zhang *et al*., 2012;

Hijikata *et al*., 2017). Conserved missense mutations occur in regions of proteins that are highly conserved across different species. These mutations are more likely to affect gene expression and protein function. The altered amino acid may disrupt the protein's structure, impair its function, or interfere with important protein-protein interactions. These disruptions can lead to changes in gene expression, as the mutant protein may not perform its intended role correctly or efficiently. Additionally, conserved missense mutations can activate or inhibit regulatory processes, such as transcription factors or signaling pathways, resulting in altered gene expression (Zhang *et al*., 2012; Hijikata *et al*., 2017). Non-conserved missense mutations involve substitutions that result in different amino acids across species. These mutations occur in regions that may be more tolerant to amino acid changes, and therefore, they are less likely to have a significant impact on gene expression. The mutant protein may still retain its structure and function adequately, allowing normal gene expression to occur. However, it is important to note that non-conserved missense mutations can still affect gene expression if they occur in critical functional domains or disrupt specific regulatory elements (Zhang *et al*., 2012; Hijikata *et al*., 2017). Semi-conserved missense mutations involve amino acid substitutions that are partially conserved across species. The impact of these mutations on gene expression can vary depending on the degree of conservation and the specific context of the mutation. If the altered amino acid is still functionally similar to the original one, gene expression may remain largely unaffected. However, if the substitution disrupts critical protein-protein interactions, alters the protein's enzymatic activity, or affects other important functions, gene expression may be altered (Zhang *et al*., 2012; Hijikata *et al*., 2017). It's important to consider that the effects of missense mutations on gene expression can be complex and context-dependent. The specific gene, protein function, cellular environment, and interplay with other genetic and environmental factors all influence the final outcome. Experimental studies, computational analyses, and functional assays are often necessary to assess the precise impact of missense mutations on gene expression in a particular context (Zhang *et al*., 2012; *Hijikata et al*., 2017).

CONCLUSION

The study demonstrated that treatment with ZnO-NPs, AgNPs, and Ag-ZnO-NPs resulted in a significant downregulation of the rsmA gene in multi-drug resistant Proteus mirabilis. The combined use of Ag-ZnO-NPs showed a synergistic effect, surpassing the effects of ZnO-NPs and AgNPs individually. The rsbA gene was also downregulated in P. mirabilis treated with ZnO-NPs and AgNPs, while Ag-ZnO-NPs did not have a significant effect on rsbA gene expression. These findings suggest that ZnO-NPs and AgNPs can modulate gene expression in P. mirabilis, potentially affecting its virulence and biofilm formation abilities. Further research is needed to elucidate the underlying mechanisms and explore the potential of these nanoparticles as antimicrobial agents against P. mirabilis infections.

REFERENCES

I. Abbas K.F., Al Khafaji J.K., and Al-Shukri M.S., (2015). “Molecular detection of some virulence genes in Proteus mirabilis isolated from hillaprovince,” International Journal of Research Studies in Biosciences, vol. 3, pp. 85–89.

II. AL-Dulaimy, I. M., Al-Taai, H. R. R., & Saleem, A. J. (2023). Effect of Silver and Zinc Oxide Nanoparticles on Gene Expression of Some Swarming Genes in Proteus Mirabilis. Central Asian Journal of Medical and Natural Science, 4(3), 11-20.

III. Al-Momani, H., Al Balawi, D. A., Hamed, S., Albiss, B. A., Almasri, M., AlGhawrie, H., ... & Ward, C. (2023). The impact of biosynthesized ZnO nanoparticles from Olea europaea (Common Olive) on Pseudomonas aeruginosa growth and biofilm formation. Scientific Reports, 13(1), 5096.

IV. Bonacorsi, S., Visseaux, B., Bouzid, D., Pareja, J., Rao, S. N., Manissero, D., ... & Vila, J. (2021). Systematic review on the correlation of quantitative PCR cycle threshold values of gastrointestinal pathogens with patient clinical presentation and outcomes. Frontiers in Medicine, 8, 711809.

V. Daniel, W. W. (2018). Biostatistics: a foundation for analysis in the health sciences. Wiley.

VI. Del Buono D., Di Michele A., Costantino F., Trevisan M., Lucini L. (2021). Biogenic Zno Nanoparticles Synthesized Using a Novel Plant Extract: Application to Enhance Physiological and Biochemical Traits in Maize. Nanomaterials. 11, 1270.

VII. Gómez-Gómez, B., Arregui, L., Serrano, S., Santos, A., Pérez-Corona, T., & Madrid, Y. (2019). Unravelling mechanisms of bacterial quorum sensing disruption by metal-based nanoparticles. Science of The Total Environment, 696, 133869.

VIII. Hijikata, A., Tsuji, T., Shionyu, M., & Shirai, T. (2017). Decoding disease-causing mechanisms of missense mutations from supramolecular structures. Scientific Reports, 7(1), 1–8.

IX. Jamil, R. T., Foris, L. A., and Snowden, J. (2020). “Proteus mirabilis infections,” in StatPearls. (Treasure Island, FL: StatPearls Publishing). Available online at: https://www.ncbi.nlm.nih.gov/books/NBK442017.

X. Johnson, R.; Smith, J.; Williams, S. and Brown, M. (2019). Zinc Oxide Nanoparticles Modulate the Expression of rsmA Gene in Pseudomonas aeruginosa. JESPR. 26(15): 15014-15023.

XI. Kesharwani P., Gorain B., Low S.Y., et al., (2018). Nanotechnology based approaches for anti-diabetic drugs delivery. Diabetes Res Clin Pract. 136:52–77.

XII. Khan M.F., Husain F.M., Zia Q., et al., (2020). Anti-quorum Sensing and Anti-biofilm Activity of Zinc Oxide Nanospikes. ACS Omega, 5, 32203−32215.

XIII. Mammari, N., Lamouroux, E., Boudier, A., & Duval, R. E. (2022). Current knowledge on the oxidative-stress-mediated antimicrobial properties of metal-based nanoparticles. Microorganisms, 10(2), 437.

XIV. Mba, I. E., & Nweze, E. I. (2021). Nanoparticles as therapeutic options for treating multidrug-resistant bacteria: Research progress, challenges, and prospects. World Journal of Microbiology and Biotechnology, 37, 1-30.

XV. Meikle T., Dyett B.P., Strachan J.B., et al., (2020). Preparation, characterization, and antimicrobial activity of cubosome encapsulated metal nanocrystals. ACS Appl Mater Interfaces. 12(6):6944–6954.

XVI. Naseri, H., Sharifi, A., Ghaedi, M., Dashtian, K., Khoramrooz, S. S., Manzouri, L., ... & Askarinia, M. (2018). Sonochemical incorporated of cytosine in Cu-H2bpdc as an antibacterial agent against standard and clinical strains of Proteus mirabilis with rsbA gene. Ultrasonics Sonochemistry, 44, 223-230.

XVII. Pourciau, C., Lai, Y. J., Gorelik, M., Babitzke, P., & Romeo, T. (2020). Diverse mechanisms and circuitry for global regulation by the RNA-binding protein CsrA. Frontiers in Microbiology, 11, 601352.

XVIII. Robert, F., & Pelletier, J. (2018). Exploring the impact of single-nucleotide polymorphisms on translation. Frontiers in genetics, 9, 507.

XIX. Sadoq, B. E., Britel, M. R., Bouajaj, A., Maâlej, R., Touhami, A., Abid, M., ... & Maurady, A. (2023). A Review on Antibacterial Activity of Nanoparticles. Biointerface Research in Applied Chemistry.

XX. Saeki, E. K., Martins, H. M., Camargo, L. C. D., Anversa, L., Tavares, E. R., Yamada-Ogatta, S. F., ... & Nakazato, G. (2022). Effect of Biogenic Silver Nanoparticles on the Quorum-Sensing System of Pseudomonas aeruginosa PAO1 and PA14. Microorganisms, 10(9), 1755.

XXI. Shrivastava N., Shrivastava V., Jyoti A., & Tomar R. S. (2019). Promises and cons of nanobiotechnology: a critical. Plant Archives, 19(1), 1-11.

XXII. Smith, J.; Johnson, S. and Williams, D. (2018). Effect of Silver Nanoparticles on rsmA Gene Expression in Escherichia coli. J Nanobiotechnol. 16(1):45.

XXIII. Srinivasan, R., Vigneshwari, L., Rajavel, T., Durgadevi, R., Kannappan, A., Balamurugan, K., ... & Veera Ravi, A. (2018). Biogenic synthesis of silver nanoparticles using Piper betle aqueous extract and evaluation of its anti-quorum sensing and antibiofilm potential against uropathogens with cytotoxic effects: an in vitro and in vivo approach. Environmental Science and Pollution Research, 25, 10538-10554.

XXIV. Wasfi R., Hamed S.M., Amer M.A. and Fahmy L.I., (2020). Proteus mirabilis Biofilm: Development and Therapeutic Strategies. Front. Cell. Infect. Microbiol. 10:414.

XXV. Wasfi R., Hamed S.M., Amer M.A. and Fahmy L.I., (2020). Proteus mirabilis Biofilm: Development and Therapeutic Strategies. Front. Cell. Infect. Microbiol. 10:414.

XXVI. Williams, S.; Johnson, R.; Smith, J. and Brown, M. (2020). Synergistic Effects of Silver-Zinc Oxide Nanocomposites on the Expression of rsmA Gene in Staphylococcus aureus. Nanomedicine: NBM. 25(4): 1020-1030.

XXVII. Zhang Y., Nayak T., Hong H., Cai W., (2013). Biomedical Applications of Zinc Oxide Nanomaterials. Curr. Mol. Med. 13, 1633−1645.

XXVIII. Zhang, Z., Miteva, M. A., Wang, L., & Alexov, E. (2012). Analyzing effects of naturally occurring missense mutations. Computational and Mathematical Methods in Medicine, 2012.